Indirect evidence for strong nonadiabatic coupling in N_2 associative desorption from and dissociative adsorption on Ru(0001)

L. Diekhöner,[a] L. Hornekær, H. Mortensen, E. Jensen, A. Baurichter, V. V. Petrunin, and A. C. Luntz[b]
Fysisk Institut, Syddansk Universitet: Odense, Campusvej 55, DK-5230 Odense M, Denmark

(Received 5 April 2002; accepted 12 June 2002)

This paper reports the simultaneous internal state and translational energy resolved associative desorption flux of N_2 from Ru(0001) using two different experimental approaches. Both experiments show that the nascent N_2 is formed with little vibrational excitation and that the total excitation in all N_2 degrees of freedom accounts for only $\frac{1}{3}$ of the barrier energy. Roughly $\frac{2}{3}$ of the energy necessary to surmount the barrier is lost to the surface in desorption. This behavior, as well as the unusual behavior noted previously in direct measurements of dissociative adsorption, both imply strong vibrational quenching in reactive trajectories passing over the high exit channel (vibrational) barrier. Adiabatic quasiclassical dynamical calculations based on the *ab initio* potential energy surface and various models of coupling to the lattice are not qualitatively consistent with N_2 vibrational damping to phonons. However, including a strong nonadiabatic coupling of the vibrational coordinate to electron–hole pairs in the dynamics does yield qualitative agreement between experiments and calculated dynamics, and we suggest this as indirect evidence for strong nonadiabatic coupling. We argue that the nonadiabatic coupling is strong in this case because of the high vibrational excitation necessary to pass over the high exit channel barrier in the reactive processes and the large charge transfer inherent in making or breaking π bonds. We believe that the same factors will be important in most activated dissociations of π bonded molecules on transition metal surfaces, e.g., for O_2, NO, N_2, and CO, and if this scenario is correct then nonadiabaticity should be important in the activated dissociation dynamics of these systems as well. [DOI: 10.1063/1.1498476]

I. INTRODUCTION

Understanding the activated dissociative adsorption of simple molecules on transition metal surfaces has been actively pursued for many years, in part because these are often rate-limiting steps in important hetereogeneous catalytic processes. For example, the activated adsorption of CH_4 is the rate-limiting step in the steam reforming of natural gas. Similarly, the dissociative adsorption of N_2 is the rate-limiting step in the Haber–Bosch synthesis of NH_3. To date, most of our fundamental concepts regarding direct activated adsorption dynamics devolves from extensive experimental and theoretical studies on the systems $H_2/Cu(111)$ and $H_2/Cu(100)$. This work has included detailed molecular beam studies of dissociative adsorption,[1,2] laser spectroscopic studies of the time-reversed process of associative desorption,[2–4] and inelastic scattering,[5,6] multidimensional density functional theory calculations (DFT) of the interaction[7,8] and many quantum and classical studies of the dynamics on model potential energy surfaces (PES)[9] and on the DFT PES.[10–12] The general picture that has emerged from this work is that the dissociation/association of H_2/Cu can be well described by two important simplifying approximations: (1) that the dynamic process is approximately electronically adiabatic, i.e., that the dynamics can be described by nuclear motion on the electronic ground state (PES) and (2) that coupling to the lattice (phonons) is minimal and can be generally ignored. Six-dimensional quantum dynamical calculations on the DFT PES are in good agreement with most aspects of the experimental details.[11] Even two-dimensional (2D) dynamical calculations on the 2D DFT PES about the optimum impact site and orientation for dissociation do give a good picture of the translational and vibrational requirements for the dissociation/association,[9] i.e., of the adiabatic barrier $V^*(0)$ and of the vibrational efficacy η_v. The simple dynamic picture from the H_2/Cu studies also works well for a qualitative discussion of CH_4 dissociation on transition metals, although coupling to the lattice cannot be ignored even qualitatively in this case due to the heavier mass of CH_4.[13]

The kinetics and dynamics of N_2 dissociation on Ru(0001) has also been actively studied for more than a decade by many groups.[14–23] Much of the motivation for this interest is that supported Ru particles are an order of magnitude more active for NH_3 synthesis than the conventional reduced Fe catalyst, and dissociative adsorption of N_2 is still the rate-limiting step. It has recently been shown, however, that the barrier to the dissociation of N_2 on Ru(0001) is dramatically lowered at steps/defects, so that these minority sites dominate thermal dissociation kinetics and hence catalytic activity.[16,17] This is undoubtedly a very general aspect

[a]Present address: Max-Planck-Institut für Festkörperforschung, D-70569 Stuttgart, Germany.
[b]Electronic mail: luntz@fysik.sdu.dk

in catalysis.[24] However, our motivation for the study of this system is largely based on the fact that N_2 dissociation on Ru(0001) terraces represents another excellent example of direct activated adsorption dynamics, with considerably different qualitative topological features than the current well-studied H_2/Cu "paradigm." For the H_2/Cu system, the adiabatic barrier $V^*(0) \approx 0.5$ eV,[7,25] and it lies mostly in the entrance channel. (By that we mean that the largest energy change in climbing the barrier occurs in the translational rather than the vibrational coordinate. For energy consumption and disposal, this is a more fundamental property than where the actual peak of the barrier is located.) On the other hand, for N_2/Ru(0001), $V^*(0) \approx 1.9$ eV, and it lies almost exclusively in the exit channel (i.e., along the vibrational coordinate).[14,19,20,22] In addition, lattice coupling will certainly be large for N_2/Ru because of the heavy molecular mass. Thus, detailed studies of the dissociative adsorption and associative desorption for N_2/Ru(0001) provide a serious test for the generality of the dynamic lessons learned from H_2/Cu (and CH_4/M, where M is a close-packed transition metal surface).

Previous molecular beam studies of the dissociative adsorption of N_2 on Ru(0001) have been recently summarized.[26] At high incident kinetic energies E, the dissociation probability S_0 is dominated by dissociation on the terraces.[27] However, there are two aspects to this dissociation behavior that seem quite unusual relative to H_2/Cu or CH_4/M dynamics. First, $S_0 \approx 0.01$ at $E \gg V^*(0)$, while for both H_2/Cu and CH_4/M $S_0 \approx 1$ at $E \gg V^*(0)$. Second, there is only a weak dependence on the initial vibrational state (or equivalently nozzle temperature T_n) for N_2/Ru, while there is a strikingly large dependence for H_2/Cu and CH_4/M. This is especially strange since there is an almost pure exit channel (vibrational) barrier for N_2/Ru, while the barriers for H_2/Cu and CH_4/M are more in the entrance channel. It was suggested previously[26] that a mechanism of energy loss to the lattice (phonons) prior to encountering the exit channel barrier could rationalize that $S_0 \approx 0.01$ at $E \gg V^*(0)$, but not the weak dependence of S_0 on the initial vibrational state. In this paper, we will suggest that the energy loss prior to encountering the barrier is to electronic degrees of freedom of the substrate rather than phonons and that this rationalizes both unusual aspects of the sticking behavior.

Associative desorption of N_2 from Ru(0001) is the time reverse of the dissociative adsorption and probes the same reactive PES. Extensive measurements of the translational energy E resolved associative desorption flux $D_f(E,T_s)$ have been presented previously using the technique of laser-assisted associative desorption (LAAD).[22] These results showed that, on average, only roughly $\frac{1}{4}$ of the barrier energy ends up in translation. It was originally suggested[20] that the low translational energy partitioning was due to strong vibrational inversion in the desorbing N_2, resulting from release of the barrier energy along the vibrational coordinate, as anticipated for an exit channel barrier, although this explanation was later recanted.[22] In this paper, we report simultaneous internal state and translationally resolved measurements of the associative desorption flux $D_f(E,v,J,T_s)$ using laser resonantly enhanced multiphoton ionization spectroscopy detection (REMPI) and two different experimental methods of preparing associatively desorbing N_2; LAAD and dissociation of a NH_3 molecular beam. Both experiments show little vibrational or rotational excitation of the associatively desorbing N_2, and individual internal states (v,J) have E distributions similar to those measured previously. Thus, there are two qualitative aspects to the associative desorption that we consider extremely unusual; (1) the low vibrational excitation in the desorbing N_2 given the high barrier along the vibrational coordinate; and (2) the fact that the N_2 desorbs with only ca. $\frac{1}{3}$ of the barrier energy, i.e., that roughly $\frac{2}{3}$ of the desorption energy is lost to the surface.

Finally, extensive ion time of flight REMPI studies of the internal state and translational energy-resolved inelastic scattering of N_2 from Ru(0001) have also recently been performed and will be reported in detail elsewhere.[28] Most aspects of this inelastic scattering seem well behaved. However, we observe little if any vibrational excitation in the scattering, i.e., $\langle \Delta E_v \rangle \approx 0$ at $E = 2.7$ eV, and this also seems unusual to us since vibrational excitation of N_2 is anticipated due to the strong curvature inherent in the 2D PES because of the exit channel barrier.[19] Such curvature generally gives strong translational to vibrational coupling and accounts for strong vibrational excitation of H_2 in inelastic scattering from Cu surfaces at high incidence energies.[5,6,29]

Thus, there are aspects to all reactive dynamic experiments for N_2 on Ru(0001) that seem unusual based on our experience of H_2/Cu (and CH_4/M) dynamics. All of the unusual aspects for the N_2/Ru(0001) reactive dynamics seem to imply strong quenching of the vibrational excitation in N_2. 3D and 4D quasiclassical dynamical calculations [translation, vibrational, and phonon coordinate(s)] based on the DFT PES[19] and various models of lattice coupling are reported here. We have tested many forms of reactive coupling to phonons, both Rayleigh and parallel surface modes, but do not find that any of these result in significant vibrational quenching of N_2 in reactive (or near reactive) trajectories. We therefore conclude that phonon coupling in electronically adiabatic dynamics is unlikely to account for the vibrational quenching and unusual behavior observed in the experiments.

On the other hand, introducing a nonadiabatic coupling of the vibrational coordinate to electron–hole pairs via a friction and fluctuating force in the 3D quasiclassical calculations does lead to quenching of the vibrational states and resolution of the unusual aspects of N_2/Ru reactive dynamics. This does, however, require quite strong nonadiabatic coupling. We suggest that strong nonadiabatic coupling is reasonable for N_2/Ru dissociation dynamics by simple analogy to the Persson and Persson model of nonadiabatic vibrational damping in chemisorbed molecules.[30] We also suggest that strong nonadiabatic coupling is likely to be generally important whenever the dissociation involves a moderate (1–2 eV) exit channel barrier and dissociation of π bonded molecules on transition metals. This includes a wide variety of important dissociation processes, e.g., dissociation of O_2, NO, CO, and N_2 on many transition metal surfaces.

II. EXPERIMENT

All associative desorption experiments reported here are performed in a molecular beamsurface science machine described in detail previously.[21,22] The Ru(0001) surface was of very high quality, with a defect density of only 0.25%. Cleaning procedures for this sample and its characterization were also described before.[21,22]

LAAD procedures are similar to those discussed earlier as well.[22] A given N coverage ($\Theta_N \approx 0.6$) is established on the Ru(0001) surface by exposing to a N atom beam. The LAAD is induced by a T jump from a pulsed ($\sim$100 ns) Alexandrite laser. Since nearly all of the associative desorption occurs at the peak of the T jump, the LAAD is well described as occurring at a fixed T_s of the peak in the T jump. This T_s is controlled by the intensity of the LAAD laser and is measured as the Boltzmann temperature characterizing the translational energy distribution of CO that is laser-induced thermally desorbed from the surface with a similar laser pulse.[22]

Typically, the LAAD induced by a few laser pulses was averaged at each spatial spot of diameter ca. 1 mm on the surface for a given experimental condition, and then the surface moved so that LAAD probed another spatial spot. The data from several spatial spots were ultimately averaged to obtain results. Some bleaching of the LAAD was observed over the scale of typically 50 laser pulses at a given spatial spot, so the bleaching rate with pulse number was measured and data corrected for this bleaching, as appropriate. The very first ca. two laser pulses on a given spatial spot often showed an anomalously high desorption intensity. Since this may originate from associative desorption of N adsorbed at residual defects (where the barrier is lower), desorption from these laser pulses was discarded in the data averaging. Slightly different schemes for data taking were employed in the various results presented in Sec. III, all chosen to minimize any systematic errors due to the variation of LAAD intensity with a spatial spot, or due to bleaching in a given spot with repeated laser pulses.

Internal states of associatively desorbing N_2 were detected via (2+1) REMPI induced by pulsed laser radiation at ca. 203 nm.[31] The laser radiation was produced by frequency tripling a commercial frequency doubled Nd:Yag pumped dye laser. The resulting REMPI radiation was ca. 1 mJ pulses, 5 ns, duration, ca. 0.1 cm^{-1} resolution and focused to a $\sim$0.1 mm diam beam parallel to the surface at distance l_{sb} from the LAAD spot on the surface. The REMPI laser was aligned to the center of the LAAD spot on the surface by translating it parallel to the surface while monitoring the REMPI intensity from N_2 formed by LAAD. The distance of the REMPI laser beam from the LAAD spot on the surface l_{sb} was then set at typically 2.7 or 4.7 mm by translating the REMPI laser beam away from the point where the REMPI laser strikes the surface. Overall alignment uncertainties in l_{sb} are estimated as 0.3 mm, and this limits the accuracy of the E scale. Because of the higher sensitivity at $l_{sb} = 2.7$ mm, this distance was used in most of the measurements reported here (e.g., comparing $v=1$ to $v=0$), despite the smaller accuracy in the E scale. The REMPI detector used in these experiment will be described in detail elsewhere.[28]

The (2+1) REMPI spectrum of N_2 consists of a set of reasonably well rotationally (J) resolved Q-branch transitions for each vibrational state v. Since this REMPI is relatively insensitive to orientation and alignment of the N_2,[32,33] the REMPI intensity $I(v,J)$ is directly proportional to the state-resolved population density or desorption density D_n by $I(v,J) \propto D_n(v,J) I_{3\omega}^2$, where $I_{3\omega}$ is the REMPI laser intensity.[28,31] This analysis was confirmed by measuring the REMPI spectrum of a hot thermal beam of N_2 of known (v,J) distributions. With the laser set to a particular Q-branch transition, translational energy distributions normal to the surface (E) for individual internal states (v,J) were obtained by measuring the time of flight from the surface to the focused REMPI laser beam by varying the delay δt between the pulsed REMPI laser and the LAAD pulsed laser inducing the T jump and associative desorption. The small time lag (ca. 30 ns) between the peak of the associative desorption and the T-jump laser was estimated from model calculations,[22] but introduced minimal changes in the energy distributions. Since the REMPI detection measures densities $D_n(\delta t, v, J, T_s)$, the results were converted to internal state and translational energy-resolved desorption fluxes as

$$D_f(E,v,J,T_s) \propto (\delta t)^2 D_n(\delta t, v, J, T_s).$$

Considerable evidence was presented earlier that LAAD measures associative desorption from terraces rather than from lower barrier defect sites.[22] The inherent low defect density of our Ru(0001) surface, the high Θ_N used in LAAD, the high T_s in LAAD (relative to TPD features at a given Θ_N) and the high-N atom diffusion barrier all minimize the role of defects in the LAAD experiment. It is also possible that residual CO adsorption and dissociation at the defects during the course of the experiments decorates them and renders them inactive. Because the first couple of laser pulses at a given spatial spot could induce desorption from N residing at low barrier defect sites, the first laser pulses were always neglected in the averaging procedure.

Because the LAAD experiments measure associative desorption at high Θ_N, we have also measured $D_f(E,v,J,T_s)$ by dissociating NH_3 on Ru(0001) at $T_s = 900$ K and used ion time of flight REMPI (TOF-REMPI) to measure the associatively desorbing N_2. The basis of the ion TOF-REMPI is to use the ion flight time following laser ionization to determine the initial velocity and hence translational energy of the neutral molecule away from the surface. In our application, the dominant component of the ion TOF is traversal through a linearly accelerating potential. With a small angular aperture ion detector, δt, the ion TOF relative to that of the peak in background $N_2(\langle E \rangle = 0)$ is $\delta t \propto \sqrt{E}$. The proportionality constant relating δt to $\sqrt{E}$ is calibrated by using seeded supersonic beams of N_2 incident on the surface, with E measured by conventional chopped beam–TOF techniques. Details of the ion TOF-REMPI detection system and its application to inelastic scattering of N_2 from Ru(0001) will be described elsewhere.[28] Because $\delta t \propto \sqrt{E}$, a different Jacobian is necessary for the flux–density transformation and $D_f(E,v,J,T_s) \propto D_n(\delta t, v, J, T_s)$.

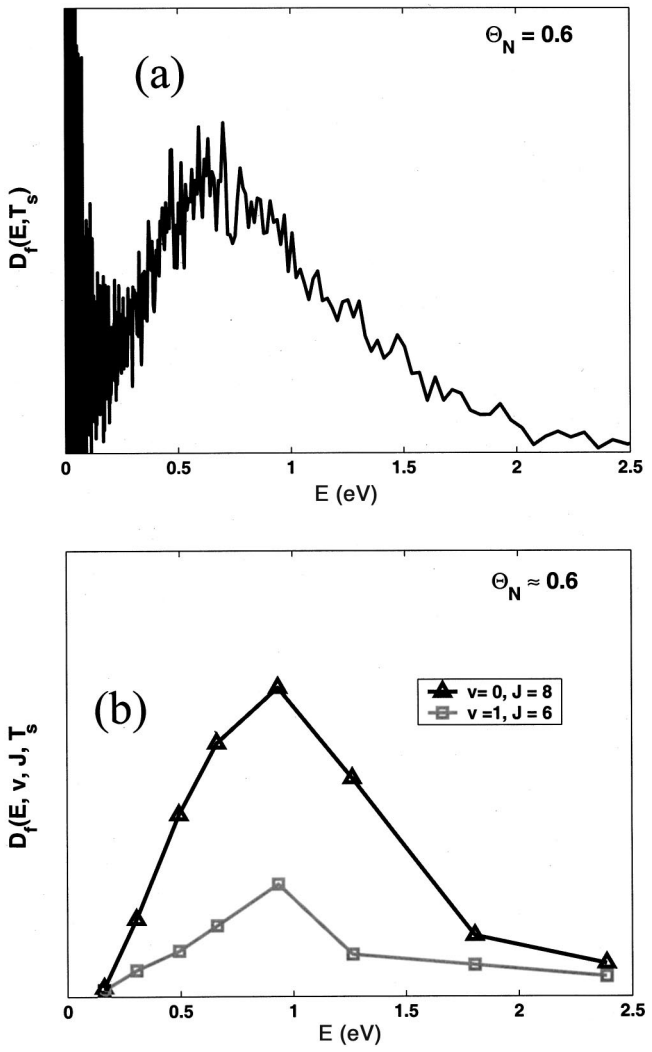

FIG. 1. (a) Associative desorption flux $D_f(E,T_s)$ of N_2 from Ru(0001) at a N coverage $\Theta_N=0.6$ as a function of normal translational energy E at $T_s \approx 875$ K. From Ref. 22. (b) Associative desorption flux $D_f(E,v,J,T_s)$ of N_2 from Ru(0001) at a N coverage $\Theta_N \approx 0.6$ at $T_s \approx 1000$ K as a function of normal translational energy E for the specific internal states $v=0$, $J=8$ and $v=1$, $J=6$.

The NH_3 was supplied as a seeded supersonic nozzle beam of NH_3 in H_2 with incident normal translation energy $E_i=1.3$ eV. At this E_i, NH_3 dissociates on the terraces with $S_0 \approx 0.15$.[34] At $T_s=900$ K, both H and N formed in the dissociation of NH_3 associatively desorb. With an estimate of the initial NH_3 flux and the known associative desorption kinetics for H_2 and N_2, we estimate that in steady state $\Theta_H < 0.01$ and $\Theta_N < 0.05$.

III. ASSOCIATIVE DESORPTION: RESULTS AND QUALITATIVE DISCUSSION

Figure 1(a) shows $D_f(E,T_s=875\,\mathrm{K})$ obtained previously by LAAD into a mass spectrometer detector for an initial $\Theta_N=0.6$.[22] In this experiment, the results are summed over all internal states produced in the associative desorption and the E scale is accurately determined. These results show a broad distribution peaking at ca. 0.7 eV, but with a tail extending up to high energies, essentially to $V^*(0)$ at the given Θ_N. The noise at $E \approx 0$ is due to convolution noise in transforming from $D_n(t,T_s)$ to $D_f(E,T_s)$. It was shown previously,[22,35] and has been discussed theoretically,[20,36] that the barrier height to dissociation is a strong function of Θ_N, although its location in the translation–vibrational (z,d) plane is largely unaffected by Θ_N. Since $V^*(0) \approx 2.9$ eV at $\Theta_N=0.6$, the average translational energy normal to the surface $\langle E \rangle$ only accounts for ca. $\frac{1}{4}$ of the available barrier energy. We initially suggested[20] that most of the remaining energy ended up in the vibrational excitation of N_2, since this was consistent with anticipated dynamics on the DFT PES.[14,19] In a subsequent more extended publication of our results,[22] we acknowledged that this original interpretation was incorrect, principally because high vibrational excitation was not observed in the state-resolved studies that will be reported below. This means that significant energy must be lost to the surface. In that extended paper,[22] we also discussed various possibilities for energy loss to the surface to account for the low $\langle E \rangle$ observed in associative desorption. It was also shown previously[22] that the shape of $D_f(E,T_s)$ is independent of T_s. This confirms that the low $\langle E \rangle$ and the distribution does not result from N_2 associative desorption from a static distribution of low barrier sites, i.e., defects.

Figure 1(b) shows $D_f(E,v,J,T_s \approx 1000\,\mathrm{K})$, obtained in LAAD with REMPI detection as outlined previously for two different v, J states: $v=0$, $J=8$ and $v=1$, $J=6$ for $\Theta_N \approx 0.6$. Each point on the curves results from a measurement of the state-resolved REMPI intensity for different delays δt between the LAAD laser and the REMPI laser.

Two striking qualitative features immediately stand out: $D_f(E,v,J,T_s \approx 1000\,\mathrm{K})$ is similar in shape to $D_f(E,T_s=875\,\mathrm{K})$ and that $D_f(E,v=1,J=6) \ll D_f(E,v=0,J=8)$, i.e., there is no vibrational inversion. Measurements also show that $D_f(E,v=2,J=8) \ll D_f(E,v=1,J=6)$ and that no higher v states were detectable. Therefore, in the release of 2.9 eV energy in associative desorption over $V^*(0)$, the average energy partitioned into N_2 vibration is very small, $\langle E_v \rangle < 0.15$ eV. This is clearly an unexpected result given the almost pure exit channel (vibrational) barrier in the PES.

Rotational state distributions were measured at a fixed E for $v=0$ by measuring relative REMPI intensities for various J states at fixed δt at $T_s \approx 1000$ K. The results were approximately described as Boltzmann distributions with a given rotational temperature T_J. We find that $T_J \approx 700$ K at $E \approx 0.3$ eV, $T_J \approx 1000$ K at $E \approx 0.9$ eV and $T_J \approx 1500$ K at $E \approx 1.8$ eV. Because of limited sensitivity, detailed rotational state distributions were not measured for $v=1$ and $v=2$, although these appeared qualitatively similar to those for $v=0$.

Despite the fact that T_J depends slightly on E, the main qualitative conclusion is that the average rotational energy $\langle E_J \rangle = \langle k_B T_J \rangle < 0.1$ eV. Thus, very little of the 2.9 eV barrier energy ends up in rotation of N_2. Within experimental error, all T_J at fixed E were the same for desorption at $T_s \approx 1400$ K as at $T_s \approx 1000$ K. Hence $\langle E_J \rangle$ was also independent of T_s.

Although detailed angular distributions were not measured for $D_f(E,v,J,T_s \approx 1000\,\mathrm{K})$, it was clear that the angular distribution was strongly peaked (ca. 20°) normal to the

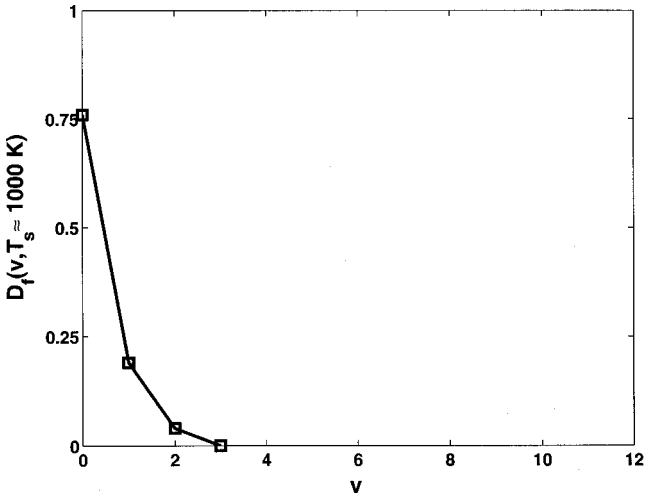

FIG. 2. Associative desorption flux $D_f(v,T_s)$ of N_2 from Ru(0001) at a N coverage $\Theta_N \approx 0.6$ at $T_s \approx 1000$ K as a function of vibrational state v. Results represent summing $D_f(E,v,J,T_s)$ over normal translational energy and rotational states.

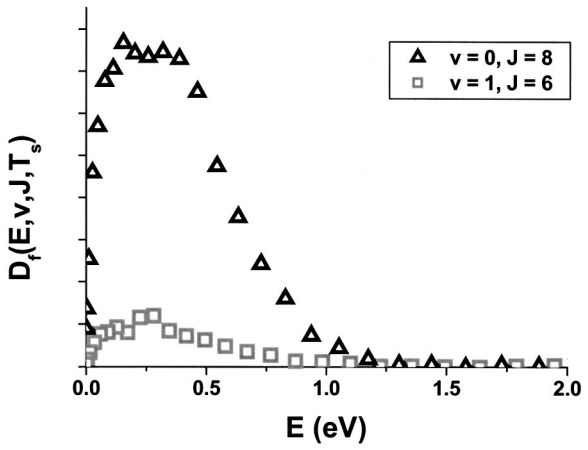

FIG. 3. Associative desorption flux $D_f(E,v,J,T_s)$ of N_2 from Ru(0001) at a N coverage $\Theta_N \approx 0.05$ produced by dissociating a high-energy beam of NH_3 at $T_s = 900$ K. Specific internal states $v=0$, $J=8$ and $v=1$, $J=6$, as in Fig. 1(b).

surface by moving the REMPI laser parallel to the surface relative to the LAAD spot irradiated on the surface. This is in complete agreement with measurements of the total associative desorption angular distribution using a mass spectrometer detector.[37] Thus, very little of the 2.9 eV barrier energy ends up in translational energy parallel to the surface, $\langle E_\parallel \rangle < 0.1$ eV.

Assuming that the rotational state distribution is the same for all v states, the relative desorption flux for each v state, summed over the E and J distributions, $D_f(v,T_s \approx 1000\ \mathrm{K})$, is given in Fig. 2. This emphasizes graphically that very little of the barrier energy ends up in N_2 vibration. Within an admittedly somewhat large statistical uncertainty, there was no dependence of the ratio $D_f(E,v=1,T_s \approx 1000\ \mathrm{K})/D_f(E,v=0,T_s \approx 1000\ \mathrm{K})$ with E. On the other hand, there was a definite measurable increase in the extent of vibrational excitation with T_s. Combining several different measurement sequences, we find that $D_f(E,v=1,J=6,T_s)/D_f(E,v=0,J=8,T_s)$ [and hence $D_f(v=1,T_s)/D_f(v=0,T_s)$] increases with T_s, with the ratio $D_f(v=1,T_s=1400\ \mathrm{K})/D_f(v=0,T_s=1000\ \mathrm{K}) = 2 \pm 1$.

In summary, the LAAD-REMPI (and previous LAAD) experiments provide rather complete information on the disposal of energy into the desorbing N_2 as a result of release of the energy of the barrier in associative desorption. There is little rotational excitation $\langle E_J \rangle < 0.1$ eV and little translational excitation parallel to the surface $\langle E_\parallel \rangle < 0.1$ eV. Both results are as anticipated. However, there is also little vibrational excitation with $\langle E_v \rangle < 0.15$, and this seems strange to us given the high exit channel barrier in the PES. Furthermore, although both the translational and rotational partitioning in associative desorption, i.e., $D_f(E,T_s)$ and $\langle E_J \rangle$, are independent of T_s, the extent of vibrational excitation, i.e., $\langle E_v \rangle$, increases moderately with T_s. This fact also seems unusual to us. Summing the channels of energy disposal into N_2, the average $\langle E + E_v + E_J + E_\parallel \rangle \approx 1\ \mathrm{eV} \ll V^*(0) \approx 2.9$ eV. Thus, on average, roughly $\frac{2}{3}$ of the energy released in associative desorption must be deposited into the surface, either into phonon modes or into electronic excitations of the surface. This is also clearly unanticipated based on H_2/Cu (or CH_4/M) dynamics.

Because the LAAD-REMPI experiments showed some very unexpected results, we have also studied N_2 associative desorption formed by NH_3 dissociation at $T_s = 900$ K. In this case, Θ_N is small so that we can check whether the unusual aspects of the LAAD-REMPI results occur because of the high Θ_N used in that technique. Results for $D_f(E,v=0,J=8,T_s=900\ \mathrm{K})$ and $D_f(E,v=1,J=6,T_s=900\ \mathrm{K})$ from NH_3 dissociation are shown in Fig. 3. The results are qualitatively similar to those from LAAD-REMPI, although both $\langle E \rangle$ and the extent of vibrational excitation are somewhat smaller than in the LAAD experiments of Fig. 1. This is anticipated since there is significantly less energy for disposal with $V^*(0) = 1.9$ eV at low Θ_N rather than 2.9 eV at $\Theta_N = 0.6$ used in the LAAD. It was shown previously[22] that $D_f(E,T_s)$ distributions shifted up considerably in E with Θ_N. There is also little rotational excitation with $T_j \approx 830$ K. Thus, the unusual results from LAAD, i.e., that $\langle E_v \rangle < 0.15$ eV and that $\langle E + E_v + E_J + E_\parallel \rangle \ll V^*(0)$ are fully confirmed in these experiments at low Θ_N as well.

Murphy *et al.*[19] also previously used NH_3 dissociation on Ru(0001) to study N_2 associative desorption by ion TOF-REMPI techniques similar to those described here. The E dependence observed by them in $D_f(E,v,J,T_s)$ is qualitatively similar to that of Fig. 3, although it peaks at somewhat lower E than that in Fig. 3. On the other hand, they assert that there is a vibrational inversion between $v=0$ and $v=1$ (dominated by the low E part of D_f). Our experiments, both those from LAAD and NH_3 dissociation, are in complete disagreement with this statement. Murphy *et al.* unfortunately do not provide the original TOF data for both v states to see how they obtained this conclusion. It has been suggested that the dominance of low E in D_f is evidence for associative desorption at lower barrier defect sites.[16] Certainly the lower Θ_N, lower T_s (relative to TPD peaks at the given Θ_N) and longer time scale for desorption make the NH_3 dissociation experiment more sensitive to defects than

LAAD.[22] It is possible (but by no means certain) that the NH_3 experiments of Murphy *et al.* are more affected by defects than ours. We have no idea of the inherent defect/impurity levels in the surface used by Murphy *et al.*, but our surface had a quite low level of defects (0.25%). We believe another difference in the two experiments is in the way the NH_3 dissociation was effected. Murphy *et al.* used thermal energy NH_3 adsorption that principally dissociates at defects through a precursor-mediated process, while we used NH_3 adsorption at $E=1.3\,\mathrm{eV}$, which principally dissociates through a direct mechanism on the terraces.[34]

IV. COMPARISON OF DYNAMICAL MODELS TO EXPERIMENTS

The observations that in associative desorption $\langle E_v \rangle < 0.15\,\mathrm{eV}$ and depends on T_s and that $\langle E+E_v+E_J+E_\parallel \rangle \ll V^*(0)$ are clearly unexpected results for dynamics on a PES with a high exit channel barrier like that for $N_2/\mathrm{Ru}(0001)$. In addition, it is difficult to rationalize based on this PES topology that in dissociative adsorption there is only a weak dependence of S_0 on nozzle temperature or equivalently v and that $S_0 \approx 0.01$ at $E \gg V^*(0)$.[26] Finally, in state-resolved inelastic scattering experiments, it is also difficult to understand the lack of vibrational excitation at $E > V^*(0)$ given the high exit channel barrier in the PES. In order to quantify this intuition, we describe below model dynamical calculations based on the *ab initio* PES and quasiclassical dynamics, and compare these with experiments. We believe that quasiclassical dynamics is an adequate treatment of the N_2 dissociation/association/scattering on Ru(0001) since it corrects approximately for a vibrational zero point and we do not anticipate that other quantum effects, e.g., tunneling, are important for the heavy N_2.

A. Adiabatic models

It is generally anticipated that dissociative adsorption and associative desorption are well described within an electronically adiabatic framework. Thus, dynamics consists of nuclear motion on the electronic ground state, i.e., on a multidimensional PES. For example, this description works extremely well for describing the many experimental studies of activated dissociation of H_2 on metals, e.g., $H_2/\mathrm{Cu}(111)$ and $H_2/\mathrm{Cu}(100)$.[11] Even two-dimensional (z,d) dynamical calculations on the 2D PES about the optimum impact site and orientation for dissociation give a good qualitative picture of the translational and vibrational requirements for the dissociation/association,[9] i.e., of the adiabatic barrier $V^*(0)$ and of the vibrational efficacy η_v.

For direct dissociation/association of heavier species, e.g., CH_4 and N_2, the same dynamic description is generally thought to be applicable, although the coupling to the lattice cannot be ignored at the outset for these heavier species. This coupling to the lattice can, at present, only be included in dissociation dynamics via some model, e.g., "dynamic recoil"[38] or as a "modified surface oscillator."[39,40] For example, CH_4 dissociation on transition metals can be qualitatively described by 3D adiabatic models, including coordinates z,d as for H_2 dynamics plus a single lattice coordinate q.[13] In this case, the inclusion of lattice coupling merely modifies the 2D dynamics by shifting the "S"-shaped 2D excitation functions to different E, increasing the width of the "S" functions and making them T_s dependent. Also, because the shift of the excitation functions, e.g., "dynamic recoil," scales with E or inversely with v, η_v increases and can in fact be greater than unity.

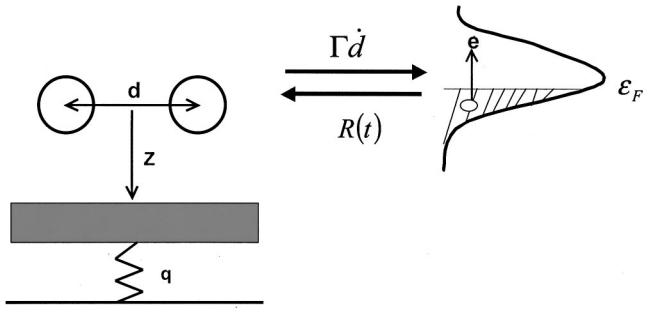

FIG. 4. Schematic diagram of the 3D model used in the quasiclassical dynamics calculations of N_2 associative desorption from and dissociative adsorption on Ru(0001). The left side of the figure gives the adiabatic model, while the right side shows the coupling of vibration to electron–hole pairs that is added in the nonadiabatic model.

Since the unusual features in the $N_2/\mathrm{Ru}(0001)$ experimental results are qualitative in nature, we focus only on a qualitative, i.e., low-dimensional theoretical description of the dynamics. In addition, the associative desorption experiments reported in Sec. III show that little of the barrier energy is partitioned in associative desorption into rotation or translational energy parallel to the surface. Therefore, we neglect those coordinates necessary to describe orientation and corrugation in the qualitative description and we are left with only the two external coordinates (z,d). The 2D PES around the optimum impact site and orientation for $N_2/\mathrm{Ru}(0001)$ dissociation is available from DFT calculations.[19] However, because N_2 is heavy, we must account for lattice coupling in any qualitative description of the $N_2/\mathrm{Ru}(0001)$ dynamics. We include this via coupling to a single Einstein oscillator, as in many previous model studies of lattice coupling in dissociation dynamics.[38–40] With only these three coordinates (z,d,q), the 3D model for the $N_2/\mathrm{Ru}(0001)$ dynamics is given on the left side of Fig. 4. In the results presented here, we take this lattice coupling as given by the "dynamic recoil" model of Hand and Harris,[38] i.e., $V_{3D}(z,d,q)=V_{2D}(z-q,d)+\frac{1}{2}kq^2$, where the second term is the harmonic lattice energy. k is chosen to give a harmonic frequency of the surface oscillator $\hbar\omega_{\mathrm{Ru}}=0.02\,\mathrm{eV}$ for a surface mass of one Ru atom.

$V_{2\text{-}D}$ was obtained by a "fit" of the DFT PES using an analytic form developed previously to describe exit channel barriers.[41] The analytic PES for dissociative adsorption had a 2.0 eV exit channel barrier ($d^{\pm}=1.80\,\text{Å}$) and was a good representation of the *ab initio* PES throughout the barrier region. No attempt was made in the analytic PES to represent the small feature corresponding to the metastable molecular state in the entrance channel since this small feature will not affect the high-energy dynamics. Because the LAAD experiments were done at $\Theta_N \approx 0.6$, where $V^*(0)$ is significantly higher,[22] two repulsion parameters in the analytic PES (V_{N_2-Ru} and V_{N-N}) were modified slightly to give

a barrier of 2.9 eV to represent the LAAD associative desorption experiments. This modified PES had essentially the identical topology to the original one, except for the higher barrier.

With this PES and the dynamic model outlined on the left side of Fig. 4, the quasiclassical dynamics are given by solving the coupled classical equations of motion for the system with total energy $E_{\mathrm{tot}}=\frac{1}{2}M_z\dot{z}^2+\frac{1}{2}M_d\dot{d}^2+\frac{1}{2}M_s\dot{q}^2+V_{3D}(z,d,q)$ and with initial conditions that satisfy quantum boundary conditions (i.e., zero point). $M_z=28$ AMU, $M_d=7$ AMU, and $M_s=101$ AMU.

Dissociation probabilities are calculated for this model by integrating Newton's equations of motion for initial conditions representing a 10 Å asymptotic molecule incident at the surface with translational energy E, vibrational energy $\hbar\omega_{N_2}(v+\frac{1}{2})$, vibrational phase ϕ_{N_2}, surface oscillator energy $\hbar\omega_{Ru}(n+\frac{1}{2})$ and vibrational phase ϕ_{Ru}. $\hbar\omega_{N_2}=0.288$ eV and $\hbar\omega_{Ru}=0.02$ eV. These initial conditions correspond to those of traditional quasiclassical trajectory approaches and many "mindless" trajectories are averaged to give final dissociation probabilities. $S_0(E,v)$ is obtained as the fraction of all trajectories with $d\geqslant 10$ Å after a significant interaction time. For a given E and v, ϕ_{N_2} and ϕ_{Ru} are chosen from a random distribution, while n is chosen according to a Boltzmann distribution at $T_s=600$ K using Metropolis Monte Carlo sampling.

The associative desorption flux $D_f(E,v,T_s)$ is calculated by assuming that transition state theory describes the associative desorption, i.e., by starting with a thermal distribution of all initial conditions along the seam separating N_2+Ru and 2N–Ru regions of the PES and integrating the equations of motion into the N_2+Ru asymptote.[42] The seam in the PES is defined as the line in the (z,d) plane perpendicular to the reaction path and passing through the transition state. Since the transition state location depends on q,q is first chosen to represent a Boltzmann distribution at T_s, i.e., with Metropolis Monte Carlo sampling of surface oscillator state n and random sampling of the vibrational phase ϕ_{Ru}. Given q, both the starting location on the seam (z^*,d^*) and the initial velocities $(\dot{z}^*,\dot{d}^*)$ on the seam are chosen by Metropolis Monte Carlo simultaneous sampling of all initial conditions so that the total initial energy into the N_2+Ru asymptote is a Boltzmann distribution at T_s. v quantum numbers and discrete values of E are assigned in the asymptotic desorption channel by conventional binning procedures of the N_2 vibrational and translational energy. For comparison with experiments, $D_f(E,T_s)=\Sigma_v D_f(E,v,T_s)$ and $D_f(v,T_s)=\Sigma_E D_f(E,v,T_s)$.

$S_0(E,v)$ from the above 3D dynamical model is given in Fig. 5 for $v=0$ and 1. The results show a sharp classical threshold for $v=0$ at $E\approx 2.5$ eV and a vibrational efficacy $\eta_v\approx 1.7$. Without lattice coupling, $S_0(E,v)$ has a threshold at $E\approx 2.0$ eV for $v=0$ and $\eta_v\approx 1.0$. The 3D adiabatic model predicts that $S_0\approx 1$ at $E\approx 3.5\,\mathrm{eV}\gg V^*(0)$ and that there should be an enormous effect of initial vibration (or T_n) due to $\eta_v\approx 1.7$.

Calculations using the "modified surface oscillator model"[39] to describe lattice coupling give qualitatively similar results to those using dynamic recoil, but with downshifted classical thresholds. Thus, independent of the details, we do not believe that this model can qualitatively rationalize the unusual behavior observed in dissociative adsorption experiments. This conclusion disagrees with our earlier suggestion that phonon coupling with an exit channel barrier would account for the low value of S_0 at high E.[26]

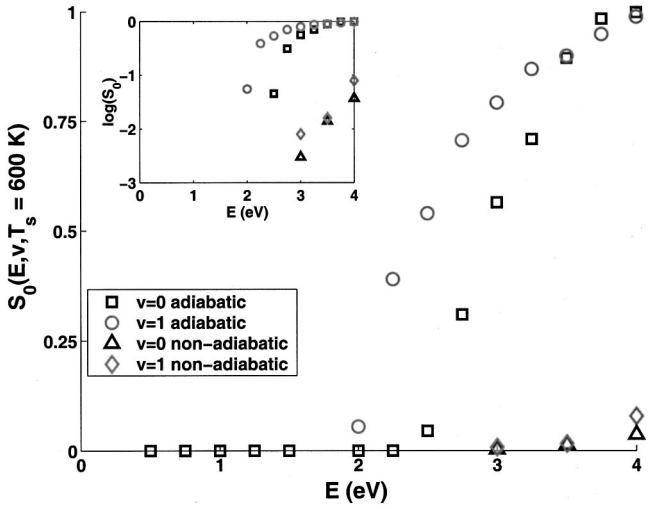

FIG. 5. Model calculations of dissociation probabilities of N_2 on Ru(0001) $S_0(E,v)$ for $v=0$ and $v=1$ as a function of translational energy E. Results for both the adiabatic and nonadiabatic models are presented as labeled in the legend. The inset shows the same calculations presented as $\log(S_0)$ vs E.

We have also calculated the extent of N_2 vibrational excitation in scattering from the surface by analyzing nonreactive trajectories. At $E=2.7$ eV, we predict significant vibrational excitation, $P(v=1)/P(v=0)\approx 0.5$, as anticipated for a high exit channel barrier and in qualitative disagreement with the experimental observation.[28] However, this disagreement must remain somewhat qualified since the nonreactive scattering samples all of phase space, i.e., all orientations of the molecule at impact and all impact sites, while the reactive trajectories presumably sample principally the minimum barrier configuration defined by the PES. Nevertheless, since H_2/Cu exhibits strong vibrational excitation at $E\approx V^*(0)$[5,6] and its barrier is considerably more toward the entrance channel than that of N_2/Ru(0001), we do consider the lack of significant vibrational excitation in N_2/Ru(0001) scattering inconsistent with the 3D adiabatic model.

$D_f(E,T_s=1000\,\mathrm{K})$ and $D_f(v,T_s=1000\,\mathrm{K})$ predicted by the adiabatic 3D model are given in Figs. 6(a) and 7(a), respectively. $D_f(E,T_s=1000\,\mathrm{K})$ peaks at $E\ll V^*(0)$ due to the preferential partitioning of the released barrier energy into vibration. The predicted $D_f(v,T_s=1000\,\mathrm{K})$ shows strong vibrational inversion, peaking at $v=6$. In addition, this model predicts that $D_f(v,T_s)$ is independent of T_s. The average energy loss to the lattice in the calculated desorption is only $\langle\Delta E_q\rangle\approx 0.15$ eV. This small value results from the preferential population of vibration in desorption, which couples only weakly to q.

The experimental observation in Fig. 1(a) is in reasonable qualitative accord with the predicted $D_f(E,T_s=1000\,\mathrm{K})$ of the 3D adiabatic model in Fig. 6(a) and it was

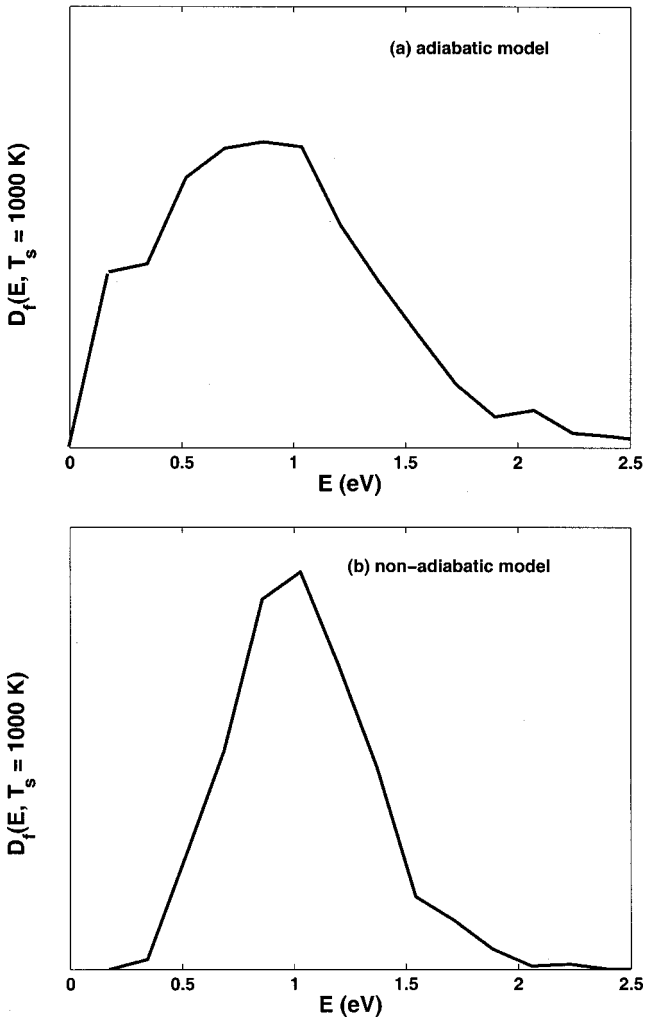

FIG. 6. Model calculations of $D_f(E,T_s=1000\ \mathrm{K})$ for N_2 associative desorption from Ru(0001). (a) Adiabatic model and (b) nonadiabatic model.

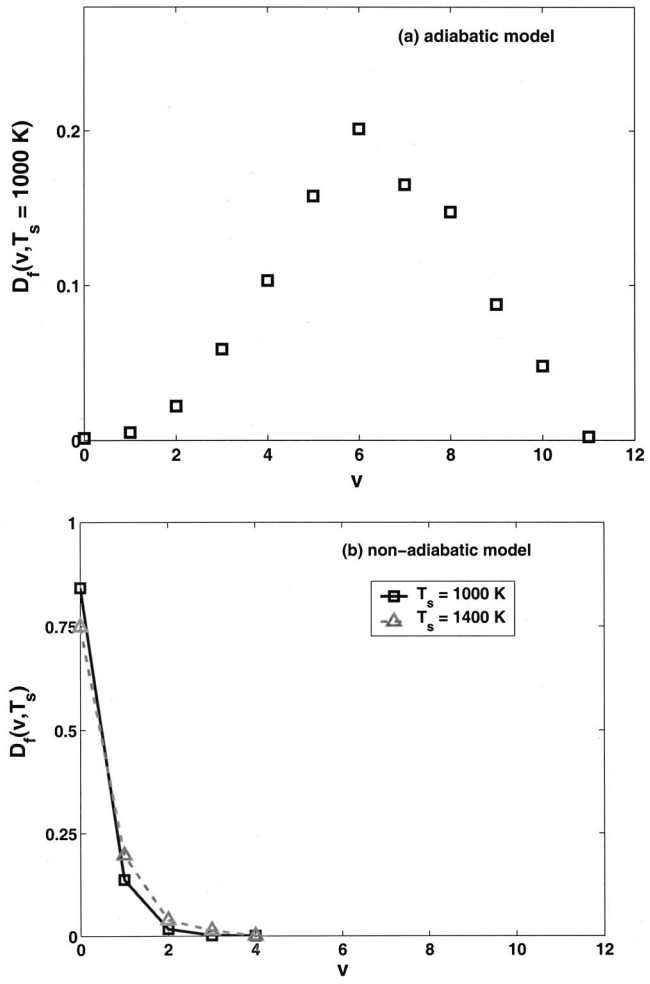

FIG. 7. Model calculations of $D_f(v,T_s)$ for N_2 associative desorption from Ru(0001) at $T_s=1000\ \mathrm{K}$ and $T_s=1400\ \mathrm{K}$. (a) Adiabatic model and (b) nonadiabatic model. There is no T_s dependence in $D_f(v,T_s)$ for the adiabatic model.

this expectation that originally encouraged us to erroneously suggest[20] the existence of strong vibrational inversion in N_2. However, the extensive vibrational inversion predicted by the 3D adiabatic model in Fig. 7(a) is in qualitative disagreement with the experimental results in Fig. 2. Hence, the unusual behavior in associative desorption, i.e., that $\langle E_v\rangle < 0.15\ \mathrm{eV}$ and that $\langle E+E_v+E_J+E_\parallel\rangle \ll V^*(0)$ [as well as the fact that $D_f(v=1,T_s)/D_f(v=0,T_s)$ changes with T_s] are all qualitatively inconsistent with adiabatic 3D dynamics.

All of the unusual experimental results in associative desorption/dissociative adsorption (and scattering) suggest that vibration is strongly quenched in a reactive interaction with the surface, and this is not present in the 3D model. Certainly, one possibility for the qualitative disagreement is that the lattice coupling is not well enough described in the 3D model. For example, the 3D model focuses on Rayleigh (perpendicular to surface) phonon coupling to the translational coordinate, as this is the term that normally dominates energy transfer to the lattice. However, phonon modes parallel to the surface $q_\parallel$ could, in principle, also couple directly to the vibrational coordinate along the reaction path and cause vibrational quenching. We have investigated several reasonable coupling mechanisms in 4D adiabatic models based on $V_{4d}(z,d,q,q_\parallel)$ (and adding the corresponding $\frac{1}{2}M_s\dot{q}_\parallel^2$ term to the kinetic energy). One such model takes $V_{4d}(z,d,q,q_\parallel)=V_{2d}(z-q,d\pm\xi(z)q_\parallel)+\frac{1}{2}kq^2+\frac{1}{2}kq_\parallel^2$, with $0<\xi(z)<1$ being a function that falls off exponentially with z and levels off to unity within the surface. Thus $\xi(z)$ accounts for the loss of coupling between d and $q_\parallel$ as the molecule leaves the surface. This form of V_{4d} was motivated to represent the fact that the electron structure in the transition state looks final-state-like and if lattice atoms move, they could drag N atoms at the transition state with them, i.e., couple directly to d. This form also represents an attempt to include ''vibrational recoil.'' We have also tried several 4D adiabatic models of the form $V_{4d}(z,d,q,q_\parallel)=V_{3d}(z,d,q)+\lambda q_\parallel+\frac{1}{2}kq_\parallel^2$, where λ is a function that depends both on z and d. A variety of forms for λ were tested, i.e., $\lambda=\lambda_0\xi\times\exp(-\alpha_0 d)$, $\lambda=\lambda_0\exp(-\alpha_0\sqrt{d^2+z^2})$ and $\lambda=\lambda_0\xi$, where λ_0 and α_0 are constants and ξ is as before. These are all essentially versions of ''modified surface oscillator'' linear coupling to the parallel phonon mode.[39] They account for a $q_\parallel$ modulation of the barrier height (and location). Such a modulation is possible due to the effects of strain on barrier heights[43] and the overall coupling strength (λ_0) was chosen

to be consistent with (static) strain-induced barrier shifts in DFT calculations.[43] Dynamic predictions of $S_0(E,v)$, $D_f(E,T_s)$ and $D_f(v,T_s)$ based on all adiabatic 4D models showed absolutely no differences to the 3D model. Vibrational excitation of $q_\parallel$ in both dissociative adsorption and associative desorption was insignificant, $\leqslant 0.03$ eV, so that the inclusion of this mode does not result in any vibrational quenching in the reactive trajectories. The finding in the 3D and 4D adiabatic models is fully consistent with the general expectation that high-frequency vibrations ω_{N_2} are only weakly damped into low-frequency phonon modes due to the high order of coupling required by the frequency mismatch. Thus, we do not believe that coupling to phonons is the cause of the N_2 vibrational quenching that seems necessary to account for all unusual features of the reactive experiments.

B. Nonadiabatic model

If coupling to phonons does not account for the vibrational quenching in reactive trajectories, then it is reasonable to suspect that coupling to electron–hole (e–h) pairs accounts for it. Nonadiabatic coupling of molecular vibrations to e–h pairs is a well-known phenomenon in surface physics. It is implicated in the damping of molecular stretching vibrations of adsorbates on metal surfaces, e.g., CO/Cu(100)[30,44,45] and O_2/Pt(111).[46] Nonadiabatic damping of vibration to e–h pairs has also been suggested as the rational for the strong multiquantum vibrational loss on scattering NO($v=15$) from a Au(111) surface.[47] In addition, the excitation of vibration from e–h pairs is the general basis suggested for substrate-mediated photochemistry and photodesorption,[48] DIMET,[49] fs-induced chemistry,[50,51] and STM-induced desorption and dissociation.[52] While many of these phenomena are often described qualitatively within a diabatic picture, i.e., of transitions between ground and excited negative ion states,[48] most quantitative treatments describe nonadiabatic couplings in terms of frictions (and fluctuating forces) added to the adiabatic dynamics.[53,54] In principle, the two approaches should yield equivalent results and merely represent a different ''basis'' to describe the nonadiabatic effects.

The nonadiabatic coupling between electronic states ψ_i and ψ_f induced by the intermolecular stretch coordinate d is $\propto \langle \psi_f | \partial/\partial d | \psi_i \rangle$. The *ab initio* calculation of these nonadiabatic terms is a formidable task and has to date only been possible for limiting models of molecule–surface systems, e.g., H_2/jellium[53,55,56] and CO/Cu clusters.[57,58] However, these few *ab initio* calculations do support the physics originally suggested in a simple model by Persson and Persson[30] as to the basis of strong vibrationally nonadiabatic coupling in the vibrational damping of chemisorbed molecules. The mechanism suggested by them involves dynamical charge transfer between the metal and the adsorbate as the molecule vibrates, with the retarded electron transfer due to the breakdown of the Born–Oppenheimer approximation causing electron–hole pair excitation. Persson and Persson used a Newns–Anderson model of the adsorbate–metal system to describe the dynamic charge transfer. As the molecule vibrates in $v=1$, the center of the adsorbate resonance ϵ_a moves up and down relative to the Fermi level ϵ_F by an amount $\delta\epsilon_a$ and induces charge transfer into the molecule $\delta n_a \approx -\rho_a(\epsilon_F)\delta\epsilon_a$, where $\rho_a(\epsilon_F)$ is the adsorbate density of states at ϵ_F and δn_a is the charge transfer over the vibrational amplitude of $v=1$. The net result is a damping into (e–h) pairs of adsorbate vibrational state $v=1$ with harmonic frequency ω with a rate $1/\tau \approx 2\pi\omega(\delta n_a)^2$. For damping from higher v states, the result is simply generalized to $1/\tau \approx 2\pi\omega v(\delta n_a)^2$. Strong damping occurs for high $E_v \approx \omega v$ and large δn_a. The latter is particularly large whenever there is a sharp structure in either the adsorbate or metal density of states. While the approximations (e.g., single adsorbate resonance, flat metal density of states, stable chemisorbed molecule) to derive the Persson and Persson formula above are unlikely to be valid for N_2/reactive dynamics, we believe the conditions for strong nonadiabatic coupling, i.e., high E_v and large δn_a, will be the same.

We introduce nonadiabatic couplings into the quasiclassical 3D dynamics model described previously by including electronic frictions and fluctuating forces in a manner identical to that discussed by Head-Gordon and Tully.[54] This is demonstrated schematically on the right side of Fig. 4. We include in the equations of motion a vibrational friction $\Gamma_d \dot{d}$ to represent damping of the vibration to e–h pairs and a randomly fluctuating force $R_d(t)$ to represent the excitation of vibration from thermally excited e–h pairs. In order to keep the surface temperature T_s fixed, the amplitude of $R_d(t)$ is chosen to satisfy the fluctuation-dissipation theorem, i.e., $\langle R_d(0)R_d(t)\rangle = (2k_B T_s \Gamma_d / M_d)\delta(t)$. Because of the randomly fluctuating $R_d(t)$, the calculation of $S_0(E,v)$ and $D_f(E,v,T_s)$ now involve averaging stochastic trajectories over the appropriate initial conditions.[54]

The friction Γ_d and hence also the fluctuating force $R_d(t)$ are implicit functions of z and d. Since we do not have *ab initio* calculations of the nonadiabatic coupling for this system and its dependence on (z,d), we simply take a functional form that is consistent with the physics implied by the Persson and Persson model,[30] i.e., that scales roughly with the charge transfer into the molecule and its variation with the coordinates (z,d). This can be inferred qualitatively by the magnitude of the induced dipole moment $\mu(z,d)$ in DFT calculations.[14] The form assumed in the calculations here is $\Gamma_d(z,d) = \Gamma_0 \xi(z) \exp[-(d-d_0)^2/2\sigma^2]$, where $\xi(z)$ is the same function used in the definition of V_{4d} and Γ_0, d_0 and σ are constants. The overall strength of nonadiabatic coupling is determined by Γ_0. The z dependence ensures that the coupling falls off essentially exponentially from the surface and yet saturates as the N_2 is fully imbedded in the metal. The d dependence centers the strength of the nonadiabatic coupling midway between the equilibrium N_2 bond length and the bond length in the transition state. This is consistent with the large change in $\mu(z,d)$ along the reaction path as the molecule stretches and approaches the transition state.[14] The detailed (z,d) dependence of the friction is largely an educated guess in the absence of *ab initio* calculations of this quantity. However, we believe the assumed form does have the right asymptotic properties and shape to scale with the charge transfer implied in the DFT calculations of $\mu(z,d)$, i.e., to

qualitatively agree with the physics described by Persson and Persson. For a fixed (z,d), the vibrational damping rate from $v=1$ to $v=0$ is related to the friction term as $(1/\tau)=[\Gamma_d(z,d)/M_d]$.

Because $\mu(z,d)$ in the DFT calculations also shows that some charge transfer occurs into the molecule as it approaches the surface, but before the N_2 bond is significantly extended, we also include a smaller friction term $\Gamma_z\dot{z}$ and corresponding fluctuating force $R_z(t)$ in the equations of motion as well. $\Gamma_z(z,d)$ was taken to have the same (z,d) form as Γ_d, but with three times smaller amplitude. Both because of the smaller amplitude and the fact that $M_z=4M_d$, the damping rate from the z coordinate was more than an order of magnitude smaller than that from the d coordinate.

$S_0(E,v)$ from the nonadiabatic model for $v=0$ and $v=1$ are given in Fig. 5. It was not feasible to calculate S_0 at lower E because averaging over too many trajectories is required to obtain the small S_0 values. Even at high $E\approx 3.5$ eV, $S_0<0.02$. In addition, the role of incident vibration is modest in determining S_0, despite the small S_0 values. Both of these qualitative results are very different from the predictions of the adiabatic model and are in qualitative agreement with the experimental observations. The qualitative interpretation for both results is that significant nonadiabatic damping of vibration occurs as the molecule climbs the barrier. Hence, the role of the incident vibration is diminished. Similarly, because of the almost pure exit channel barrier, dissociation principally occurs by transferring $E\rightarrow v$ by curvature along the reaction path. When v is also simultaneously damped as N_2 tries to surmount the barrier, S_0 approaches unity very slowly with increasing E, and it is still small at $E=3-4$ eV. Neglect of the z damping term in the nonadiabatic model does shift the upturn in S_0 with E to slightly lower E. For example, $S_0\approx 0.1$ at $E=3.5$ eV without z damping. We also suspect that inclusion in the model dynamics of an angular coordinate of the N_2 axis relative to the surface would also decrease S_0 at high E as well, especially for the high exit channel barrier of N_2/Ru(0001).[9,11]

Vibrational excitation $[P(v>0)]$ in scattering at high E is also fully quenched in the nonadiabatic model, in qualitative agreement with the experimental result. The $E\rightarrow v$ excitation caused by reaction path curvature in the scattering trajectory is simultaneously damped via excitation of (e–h) pairs. Of course, a quantitative treatment of scattering must go beyond a 3D dynamic model.

$D_f(E,T_s=1000\,\mathrm{K})$ predicted by the nonadiabatic model is given in Fig. 6(b). This is narrowed slightly relative to the adiabatic model, but is still in good qualitative agreement with the experimental results of Fig. 1. Neglect of the z-dependent damping term shifts the peak of this distribution $\sim$0.25 eV to higher E.

$D_f(v,T_s)$ from the nonadiabatic model is given in Fig. 7(b) for $T_s=1000$ K and $T_s=1400$ K. In contrast to the adiabatic model, $\langle E_v\rangle$ is now very small because of the strong nonadiabatic damping of vibration as the molecule descends the barrier and desorbs. This is in very good agreement with the experimental results presented in Fig. 2. In addition, the extent of vibrational excitation in the desorbed N_2 is predicted to depend moderately on T_s, again in very good qualitative agreement with the experiment. The origin of this T_s dependence in the model is the term $R_d(t)$, which describes vibrational heating due to thermally excited (e–h) pairs. Because the nonadiabatic coupling to z was more than an order of magnitude smaller than that to d in the model, $D_f(E,T_s)$ was predicted to be nearly independent of T_s, in agreement with experiment.[22] We also note that calculated values of $D_f(v,T_s)$ were completely independent of whether or not damping was present along z.

We wish to emphasize that the model developed here is very different in spirit and physics to the diabatic model proposed by Kosloff and collaborators.[23] Their model treats the "nonadiabatic" coupling between a molecular physisorbed PES and a dissociated atomic PES. It is a fully elastic theory that does not account for any damping of energy into either the lattice or into e–h pairs. This model was constructed to account for the fact that $S_0\ll 1$ at high E. However, the diabatic PES and the seam between them that they found necessary to fit the sticking results bears little resemblance to the DFT PES, i.e., it is dominated by an *entrance* channel seam (barrier).

V. IMPLICATIONS OF THE NONADIABATIC COUPLING

In summary, we cannot obtain qualitative agreement of any adiabatic dynamic model with the unusual experimental results for $D_f(v,T_s)$ and $S_0(E,v)$, while the model incorporating nonadiabatic coupling of the vibrational coordinate to (e–h) pairs gives good qualitative agreement. We take this as *indirect evidence* that N_2 associative desorption from and dissociative adsorption on Ru(0001) is dominated by nonadiabatic effects. However, to achieve agreement between the nonadiabatic model and experiment requires that the magnitude of the nonadiabatic coupling Γ_0 be extremely strong, so that $\langle 1/\tau\rangle\approx\frac{1}{20}$ fs^{-1}, with $\langle\ \rangle$ representing averaging the reactive trajectory from the entrance channel to the transition state, or *vice versa*. This strong coupling is required to extensively damp the vibrational coordinate on its reactive path to/from the transition state. This coupling is, in fact, so strong that a friction approximation may not be quantitatively appropriate.[54] However, since it is virtually impossible to go beyond such an approximation and we are primarily concerned with a qualitative explanation for the unusual reactive N_2/Ru(0001) behavior, we neglect this potential difficulty.

Whether such a strong nonadiabatic coupling is physically reasonable is, of course, the key question and cannot be answered until there is an *ab initio* calculation of the nonadiabatic coupling or $\Gamma_d(z,d)$ for this system. In general, knowledge of the strength of nonadiabatic couplings between vibration and (e–h) pairs is quite limited for all systems. A few examples exist for the vibrational damping rate from $v=1$ of stable molecular adsorbates, e.g., from direct fs measurement of the vibrational lifetime[45] or indirectly inferred via the vibrational linewidth.[44,46] For example $1/\tau\approx\frac{1}{1000}$ fs^{-1} for $CO(v=1)/Cu(100)$[45] and $1/\tau\approx\frac{1}{250}$ fs^{-1} for $O_2(v=1)/Pt(111)$.[46] The O_2/Pt(111) analogy is probably closest to N_2/Ru(0001) reactive trajectories since this adsorbate also represents a π-bonded molecule parallel to the surface

as in the N_2/Ru transition state. The overall vibrational damping rate necessary to rationalize the N_2/Ru reactive dynamics is, however, even an order of magnitude larger than that of $O_2(v=1)$/Pt(111). While it is impossible to really compare nonadiabatic damping in reactive trajectories with that of chemisorbed species, we note that the Persson and Persson model of vibrational damping gives $1/\tau \approx 2\pi\omega v(\delta n_a)^2$. For O_2/Pt(111) vibrational damping, $\hbar\omega=0.1$ eV, $v=1$, and $\delta n_a \approx 0.15e$ from the above model equation to fit the measured decay rate of $v=1$. For N_2/Ru, dissociative adsorption or associative desorption, $\omega=0.29$ eV and $\langle v\rangle \approx 6$. Thus, if δn_a is comparable to that in O_2/Pt, then the vibrational damping rate of a N_2 molecule hypothetically frozen midway through the dissociation/association should be an order of magnitude larger in N_2/Ru reactive trajectories than for $O_2(v=1)$ stably adsorbed on Pt(111). A rough estimate of δn_a is available from the dipole moment change upon stretching the molecule along the reaction path, $\Delta\mu \approx \delta n_a \langle Z\rangle$, where $\langle Z\rangle$ is the distance of charge transfer, i.e., the distance between the center of the N_2 π orbital and the image plane. Taking the latter as half a lattice spacing gives $\langle Z\rangle \approx 0.2$ Å. Since $\Delta\mu \approx 0.10$ D (over a distance comparable to the $v=1$ vibrational amplitude) from the DFT calculations as the molecule climbs the activation barrier,[14] we obtain $\delta n_a \approx 0.10e$, roughly as large as for the O_2/Pt(111) case. While this estimate is very heuristic, it does suggest that there is significant charge transfer inherent in dissociative adsorption/associative desorption of N_2/Ru as evidenced by the large $\Delta\mu$ and small $\langle Z\rangle$ in the DFT calculations.

There are many factors that we believe conspire to make the nonadiabatic coupling strong in N_2/Ru reactive trajectories. First, the high exit channel barrier means that high vibrational excitation must be involved in the dissociation/desorption, and $\langle 1/\tau\rangle$ scales with this excitation. Second, there is significant charge transfer involved in stretching the bond, i.e., climbing the barrier, because the dissociation (desorption) breaks (makes) multiple π bonds when the N_2 is parallel to and very close to the surface. We anticipate that exactly these same factors will be important for a large class of other molecular dissociations as well, i.e., whenever the dissociation of π-bonded molecules has a significant exit channel barrier. Thus, we suggest that nonadiabatic coupling could be important in reactive dynamics for these systems as well. This dynamic scenario describes a wide class of important molecular dissociation process; O_2, NO, CO, and N_2 activated dissociations on many transition metals, since when barriers exist, they are invariably almost pure exit channel barriers.[59] We therefore suggest that the inclusion of nonadiabatic couplings in a qualitative description of the reactive dynamics of these systems may be necessary. Clearly, difficult *ab initio* calculations of the nonadiabatic coupling terms will be necessary to prove or disprove this suggestion.

Although the most extensive experimental (and theoretical) results are now available for N_2 reactive dynamics on Ru(0001), other N_2/metal systems to do show evidence of unusual dynamic behavior as well. For example, vibrational excitation seems rather low in N_2 associative desorption from all transition metals given the high exit channel barriers.[60,61] In associative desorption of N_2 from Cu(111),[61,62] all modes of N_2 excitation $(E,v,J,E_\parallel)$ have been measured via techniques similar to those described here. In this case, $\langle E+E_v+E_J+E_\parallel\rangle \ll V^*(0)$ as well. Evidence of unusual reactive behavior for other molecular systems is far less persuasive at this time. However, we do note that it does not seem possible to dissociate directly (at low T_s) many π-bonded molecules with exit channel barriers (except at steps and defects), even with $E \gg V^*(0)$, e.g., O_2/Pt(111),[63] O_2/Ag(111) and Ag(100),[64,65] CO/Ru(0001),[66] etc. We suggest that part of the difficulty in direct dissociation of these systems results from vibrational damping caused by nonadiabatic coupling.

If the nonadiabatic coupling and vibrational damping is as generally strong as we suggest, then this mechanism could also be important in inhibiting dissociation of π-bonded molecules on large metal catalyst particles. However, on small metal particles (ca. <2.5 nm), the nonadiabatic vibrational damping is likely to be ineffective due to the low density of e–h pair states.[67] The variation in the importance of this mechanism with particle size may prove to be another aspect of the particle size dependence in catalysis.

The activated dissociations of H_2/Cu and CH_4/M seem well described within an adiabatic framework. This is entirely consistent with the factors suggested above as to what causes strong nonadiabatic vibrational couplings. The barriers for H_2/Cu and CH_4/M are largely in the entrance rather than the exit channel. Hence, only modest vibrational excitation is required (produced) in adsorption (desorption). Secondly, the breaking/making of a single σ bond relatively far from the surface (because of the entrance channel character of the barrier) involves only modest charge transfer. Thus, we believe that nonadiabatic effects for the activated dissociation of π-bonded molecules may well be more than an order of magnitude larger than that for H_2/Cu and CH_4/M dissociations, despite the smaller vibrational reduced masses of the latter.

VI. SUMMARY AND CONCLUSIONS

In this paper we present internal state and translational energy-resolved measurements of N_2 associative desorption from Ru(0001) using the technique of LAAD with REMPI detection. These experiments measure the partitioning of energy into N_2 as it descends the barrier from the transition state. We find that little energy is partitioned into rotation E_J, translational energy parallel to the surface $E_\parallel$, and surprisingly even vibration E_v. The state-resolved translational energy E distributions are broad, with a high-energy tail extending to the barrier $V^*(0)$. There are three aspects to these results that we consider unusual based on anticipated dynamics on the PES, i.e., that $\langle E_v\rangle < 0.15$ eV, that $\langle E_v\rangle$ depends on T_s, and that $\langle E+E_\parallel+E_v+E_J\rangle \approx \frac{1}{3}V^*(0)$. The latter means that nearly $\frac{2}{3}$ of the energy released in descending the barrier is lost to the surface. Because LAAD studied associative desorption at high Θ_N, we have also produced N_2 associative desorption at low Θ_N by dissociating a high-energy beam of NH_3 at high T_s. Ion TOF-REMPI detection measures E, E_v, and E_J in the associative desorption and confirms the unusual results observed in LAAD. In addition to

these unusual aspects in associative desorption, it was pointed out previously[26] that there are also two unusual observations in molecular beam measurements of dissociative adsorption S_0, i.e., that $S_0 \ll 1$ at $E \gg V^*(0)$ and that S_0 is only a weak function of the nozzle temperature (or equivalently of vibrational state v). We also note that no measurable vibrational excitation is observed in inelastic scattering at $E \geqslant V^*(0)$, and this seems unusual to us given the exit channel nature of the barrier in the PES.

All unusual experimental results seem to imply that there is strong vibrational quenching in the reactive (or near-reactive) dynamics. We have examined several 3D and 4D models of the adiabatic dynamics, based on the *ab initio* DFT PES and various assumptions about coupling to the lattice (phonons). We do not observe any significant vibrational damping to phonons in any of these models, and hence any qualitative resolution of the unusual experimental results. On the other hand, including a nonadiabatic coupling of the vibration to electron–hole pairs via a friction and fluctuating force does produce vibrational damping and a good qualitative resolution of all unusual experimental results. It does, however, require quite strong nonadiabatic coupling. We believe this strong coupling is reasonable based on analogy to the Persson and Persson model of vibrational damping of adsorbates.[30] We take the inability of any adiabatic model to qualitatively describe the experiments, while a nonadiabatic model does, as *indirect evidence* for strong nonadiabatic coupling in the reactive dynamics.

We suggest that the factors that we believe make nonadiabatic coupling strong in this case will be quite general, and will most likely make nonadiabatic coupling important whenever π-bonded molecules dissociate on a metal and have a high exit channel barrier. This includes a wide variety of important activated dissociation processes, e.g., O_2, NO, CO, N_2 dissociation on many transition metals. There is some evidence that reactive events in some of these systems also exhibit unusual dynamic behavior.

Hopefully, realistic *ab initio* calculations of the nonadiabatic coupling $\Gamma_d(z,d)$ will be forthcoming in the near future to test the hypothesis presented here.

ACKNOWLEDGMENTS

The authors acknowledge support of this work by the Danish Research Council under Grant No. 9601724 and 51000269. Two of the authors (H.M. and L.D.) thank the Danish Research Academy for support during their Ph.D. studies and L.H. wishes to acknowledge support from the Carlsberg Fond. We also wish to thank P. Saalfrank for originally making us aware that the vibrational damping inherent in the Persson and Persson model scales with the vibrational energy.

[1] C. T. Rettner, D. J. Auerbach, and H. A. Michelsen, Phys. Rev. Lett. **68**, 1164 (1992).
[2] C. T. Rettner, H. A. Michelsen, and D. J. Auerbach, J. Chem. Phys. **102**, 4625 (1995).
[3] H. A. Michelsen, C. T. Rettner, D. J. Auerbach, and R. N. Zare, J. Chem. Phys. **98**, 8294 (1993).
[4] H. Hou, S. J. Gulding, C. T. Rettner, A. M. Woodtke, and D. J. Auerbach, Science **277**, 80 (1997).
[5] C. T. Rettner, D. J. Auerbach, and H. A. Michelsen, Phys. Rev. Lett. **68**, 2547 (1992).
[6] A. Hodgson, J. Moryl, P. Traversaro, and H. Zhao, Nature (London) **356**, 501 (1992).
[7] B. Hammer, M. Scheffler, K. W. Jacobsen, and J. K. Nørskov, Phys. Rev. Lett. **73**, 1400 (1994).
[8] G. J. Kroes, E. J. Baerends, and R. C. Mowrey, J. Chem. Phys. **107**, 3309 (1997).
[9] G. R. Darling and S. Holloway, Rep. Prog. Phys. **58**, 1595 (1995).
[10] D. A. McCormack, G.-J. Kroes, R. A. Olsen, E.-J. Baerends, and R. C. Mowrey, J. Chem. Phys. **110**, 7008 (1999).
[11] G. J. Kroes, Prog. Surf. Sci. **60**, 1 (1999).
[12] A. Gross and M. Scheffler, Phys. Rev. B **57**, 2493 (1998).
[13] A. C. Luntz and J. Harris, Surf. Sci. **258**, 397 (1991).
[14] J. J. Mortensen, Y. Morikawa, B. Hammer, and J. K. Nørskov, J. Catal. **169**, 85 (1997).
[15] J. J. Mortensen, Y. Morikawa, B. Hammer, and J. K. Nørskov, Z. Phys. Chem. (Leipzig) **198**, 113 (1997).
[16] S. Dahl, A. Logadottir, R. C. Egeberg, J. H. Larsen, I. Chorkendorff, E. Törnqvist, and J. K. Nørskov, Phys. Rev. Lett. **83**, 1814 (1999).
[17] S. Dahl, E. Törnqvist, and I. Chorkendorff, J. Catal. **192**, 381 (2000).
[18] K. Jacobi, Phys. Status Solidi A **177**, 37 (2000).
[19] M. J. Murphy, J. F. Skelly, A. Hodgson, and B. Hammer, J. Chem. Phys. **110**, 6954 (1999).
[20] L. Diekhöner, H. Mortensen, A. Baurichter, A. C. Luntz, and B. Hammer, Phys. Rev. Lett. **84**, 4906 (2000).
[21] L. Diekhöner, A. Baurichter, H. Mortensen, and A. C. Luntz, J. Chem. Phys. **112**, 2507 (2000).
[22] L. Diekhöner, H. Mortensen, A. Baurichter, and A. C. Luntz, J. Chem. Phys. **115**, 3356 (2001).
[23] L. Romm, G. Katz, R. Kosloff, and M. Asscher, J. Phys. Chem. B **101**, 2213 (1997).
[24] J. K. Nørskov, T. Bligaard, A. Logadottir *et al.*, J. Catal. (in press).
[25] G. Wiesenekker, G. J. Kroes, and E. J. Baerends, J. Chem. Phys. **104**, 7344 (1996).
[26] L. Diekhöner, H. Mortensen, A. Baurichter, E. Jensen, V. Petrunin, and A. C. Luntz, J. Chem. Phys. **115**, 9028 (2001).
[27] R. C. Egeberg, J. H. Larsen, and I. Chorkendorff, Phys. Chem. Chem. Phys. **3**, 2007 (2001).
[28] H. Mortensen, E. Jensen, A. Baurichter, L. Diekhöner, V. V. Petrunin, and A. C. Luntz (unpublished).
[29] G. R. Darling and S. Holloway, J. Electron Spectrosc. Relat. Phenom. **64-5**, 571 (1993).
[30] B. N. J. Persson and M. Persson, Solid State Commun. **36**, 175 (1980).
[31] K. R. Lykke and B. D. Kay, J. Chem. Phys. **95**, 2252 (1991).
[32] T. F. Hanisco and A. C. Kummel, J. Phys. Chem. **95**, 8565 (1991).
[33] T. F. Hanisco, C. Yan, and A. C. Kummel, J. Phys. Chem. **96**, 2982 (1992).
[34] H. Mortensen, L. Diekhöner, A. Baurichter, E. Jensen, and A. C. Luntz, J. Chem. Phys. **113**, 6882 (2000).
[35] L. Diekhöner, H. Mortensen, A. Baurichter, and A. C. Luntz, J. Vac. Sci. Technol. A **18**, 1509 (2000).
[36] B. Hammer, Phys. Rev. B **63**, 205423 (2001).
[37] T. Matsushima, Surf. Sci. **197**, L287 (1988).
[38] M. Hand and J. Harris, J. Chem. Phys. **92**, 7610 (1990).
[39] M. Dohle and P. Saalfrank, Surf. Sci. **373**, 95 (1997).
[40] M. Dohle, P. Saalfrank, and T. Uzer, Surf. Sci. **409**, 37 (1998).
[41] A. C. Luntz, J. Chem. Phys. **102**, 8264 (1995).
[42] J. Harris, S. Holloway, T. S. Rahman, and K. Yang, J. Chem. Phys. **89**, 4427 (1988).
[43] M. Mavrikakis, B. Hammer, and J. K. Nørskov, Phys. Rev. Lett. **81**, 2819 (1998).
[44] R. Ryberg, Phys. Rev. B **32**, 2671 (1985).
[45] M. Morin, N. N. Levinos, and A. L. Harris, J. Chem. Phys. **96**, 3950 (1992).
[46] B. N. J. Persson, Chem. Phys. Lett. **139**, 457 (1987).
[47] Y. H. Huang, C. T. Rettner, D. J. Auerbach, and A. M. Wodtke, Science **290**, 111 (2000).
[48] J. W. Gadzuk, L. J. Richter, S. A. Buntin, D. S. King, and R. R. Cavanagh, Surf. Sci. **235**, 317 (1990).
[49] T. F. Heinz, J. A. Misewich, M. M. T. Loy, D. M. Newns, and H. Zacharias, Springer Ser. Surf. Sci. **31** (DIET V Proceedings), 47 (1993).
[50] M. Bonn, S. Funk, C. Hess, D. N. Denzler, C. Stampfl, M. Scheffler, M. Wolf, and G. Ertl, Science **285**, 1042 (1999).

[51] C. Hess, S. Funk, M. Bonn, D. N. Denzler, M. Wolf, and G. Ertl, Appl. Phys. A: Mater. Sci. Process. **71**, 477 (2000).
[52] B. C. Stipe, M. A. Rezaei, W. Ho, S. Gao, M. Persson, and B. I. Lundqvist, Phys. Rev. Lett. **78**, 4410 (1997).
[53] B. Hellsing, M. Persson, and B. I. Lundqvist, Surf. Sci. **126**, 147 (1983).
[54] M. Head-Gordon and J. C. Tully, J. Chem. Phys. **103**, 10137 (1995).
[55] M. Persson and B. Hellsing, Phys. Rev. Lett. **49**, 662 (1982).
[56] B. Hellsing and M. Persson, Phys. Scr. **29**, 360 (1984).
[57] T. T. Rantala, A. Rosen, and B. Hellsing, J. Electron Spectrosc. Relat. Phenom. **39**, 173 (1986).
[58] M. Head-Gordon and J. C. Tully, J. Chem. Phys. **96**, 3939 (1992).
[59] M. Mavrikakis, L. B. Hansen, J. J. Mortensen, B. Hammer, and J. K. Nørskov, ACS Symp. Ser. **721**, 245 (1999).
[60] R. P. Thorman and S. L. Bernasek, J. Chem. Phys. **74**, 6498 (1981).
[61] M. J. Murphy, J. F. Skelly, and A. Hodgson, Chem. Phys. Lett. **279**, 112 (1997).
[62] M. J. Murphy, J. F. Skelly, and A. Hodgson, J. Chem. Phys. **109**, 3619 (1998).
[63] C. T. Rettner and C. B. Mullins, J. Chem. Phys. **94**, 1626 (1991).
[64] F. Buatier de Mongeot, U. Valbusa, and M. Rocca, Surf. Sci. **339**, 291 (1995).
[65] U. Valbusa, F. B. De Mongeot, M. Rocca, and L. Vattuone, Vacuum **50**, 445 (1998).
[66] S. Kneitz, J. Gemeinhardt, and H.-P. Steinruck, Surf. Sci. **440**, 307 (1999).
[67] E. Blaisten-Barojas and J. W. Gadzuk, J. Chem. Phys. **97**, 862 (1992).